First principles study of the electronic structure and bonding of Mn_2

Demeter Tzeli,[1] Ulises Miranda,[2] Ilya G. Kaplan,[2,a)] and Aristides Mavridis[3,b)]
[1]*Theoretical and Physical Chemistry Institute, National Hellenic Research Foundation, 48 Vassileos Constantinou Ave., Athens 116 35, Greece*
[2]*Instituto de Investigaciones en Materiales, Universidad Nacional Autónoma de México, Apdo. Postal 70-360, 04510 México, D.F., Mexico*
[3]*Laboratory of Physical Chemistry, Department of Chemistry, National and Kapodistrian University of Athens, P.O. Box 64 004, 157 10 Zografou, Athens, Greece*

(Received 9 July 2008; accepted 15 September 2008; published online 17 October 2008)

We have examined the electronic structure and bonding of the Mn_2 molecule through multireference variational calculations coupled with augmented quadruple correlation consistent basis sets. The Mn atom has a $^6S(4s^2 3d^5)$ ground state with its first excited state, $^6D(4s^1 3d^6)$, located 2.145 eV higher. For all six molecular states $^1\Sigma_g^+$, $^3\Sigma_u^+$, $^5\Sigma_g^+$, $^7\Sigma_u^+$, $^9\Sigma_g^+$, and $^{11}\Sigma_u^+(1)$ correlating to $Mn(^6S)+Mn(^6S)$, and for six undecets, i.e., $^{11}\Pi_u$, $^{11}\Sigma_g^+$, $^{11}\Delta_g$, $^{11}\Delta_u$, $^{11}\Sigma_u^+(2)$, and $^{11}\Pi_g$ with end fragments $Mn(^6S)+Mn(^6D)$, complete potential energy curves have been constructed for the first time. We prove that the bonding in Mn_2 dimer is of van der Waals type. The interaction of two Mn ^6S atoms is hardly influenced by the total spin, as a result the six Σ states, singlet ($^1\Sigma_g^+$) to undecet ($^{11}\Sigma_u^+(1)$), are in essence degenerate packed within an energy interval of about 70 cm^{-1}. Their ordering follows the spin multiplicity, the ground state being a singlet, $X\ ^1\Sigma_g^+$, with binding energy D_e (D_0) ≈ 600 (550)cm^{-1} at $r_e \approx 3.60$ Å. The six undecet states related to the $Mn(^6S)+Mn(^6D)$ manifold, are chemically bound with binding energies ranging from 3 ($^{11}\Pi_g$) to 25 ($^{11}\Pi_u$)kcal/mol and bond distances about 1 Å shorter than the states of the lower manifold, $Mn(^6S)+Mn(^6S)$. The lowest of the undecets is of Π_u symmetry located 30 kcal/mol above the $X\ ^1\Sigma_g^+$ state. © *2008 American Institute of Physics*. [DOI: 10.1063/1.2993750]

I. INTRODUCTION

First row transition metal clusters have attracted lately a great deal of attention both experimentally and theoretically; among them manganese clusters are the most frequently studied. The special interest on manganese systems is connected with their unusual magnetic properties depending on their environment.[1,2] The ground state of Mn is ^6S ($3d^5 4s^2$) with the first excited state ^6D ($3d^6 4s^1$) located 2.145 eV higher.[3] Solid Mn, known as *a*-Mn, is antiferromagnetic and has a very complex lattice structure with 54 atoms per unit cell, while dilute "solutions" of Mn in Cu behave like spin glasses.[4] The unusual magnetic behavior of Mn systems appears as well in the nanoscale range in the case of Mn clusters.[5–8] For instance, the electron spin resonance (ESR) studies of Mn_2 and Mn_5 in rare-gas matrices, revealed that Mn_2 has an antiferromagnetic ground state with $S=0$, whereas Mn_5 has a ferromagnetic ground state with all spins parallel and $S=25/2$.[5]

The simplest Mn system, the dimer Mn_2, shows some interesting features different from other 3*d*-transition metal dimers. For example, the interatomic distance r_e in Mn_2 is estimated to be 3.4 Å,[5,6] quite larger than that in bulk (2.25–2.95 Å), while in the case of all other 3*d*-transition metal dimers the situation is the opposite. ESR (Ref. 6) studies on Mn_2 showed that there is a kind of *exchange restriction*, previously observed in solids and named *magnetostriction*,[9] leading to a strong dependence of the equilibrium distance on *S*. For $S=0-5$ r_e varies from 3.2 to 3.6 Å.

The analysis of the ESR spectrum in Refs. 5 and 6 was based on the Landé expression[10]

$$E(S) = -\frac{J}{2}[S(S+1) - s(s+1)], \tag{1}$$

where *J* is the exchange coupling constant, *S* the total spin of the dimer, and *s* the atomic spin. Expression (1) is the eigenenergy of the Heisenberg exchange Hamiltonian

$$\hat{H} = -J\,\hat{S}_a \cdot \hat{S}_b, \tag{2}$$

where $\hat{S}_a$ and $\hat{S}_b$ are the spin operators of atoms *a* and *b*, respectively. From Eq. (1) follows the so-called Landé interval rule

$$\Delta_{S,S-1} = E(S) - E(S-1) = -J \cdot S, \tag{3}$$

namely, the difference between adjacent spin states is proportional to the value of the total spin. From ESR measurements on Mn_2 it was found that $J=-9\pm 3$ cm^{-1};[5] ultraviolet and Raman spectroscopy give a similar value $J=-10\pm 0.6$ cm^{-1}.[11]

The dissociation energy (D_e) of Mn_2 was estimated for the first time in 1968 through mass spectrometry by Kant *et al.*[12] Using the third law of thermodynamics and a van der Waals model these authors obtained $D_e=0.33\pm 0.26$ eV.

a)Electronic mail: kaplan@iim.unam.mx.
b)Electronic mail: mavridis@chem.uoa.gr.

Twenty years later Haslett *et al.*[13] based on the same mass spectrometric data[12] and the van der Waals model, but using more recent molecular parameters, obtained D_e=0.02 eV. On the other hand, by applying the LeRoy–Bernstein procedure[14] they extracted D_e=0.15 eV.[13] A value of D_e=0.44±0.30 eV was reported by Gingerich[15] based on the third law of thermodynamics, while a D_0=0.6±0.1 eV was indirectly determined from measurements on charged Mn_x^+ (x=3, 4) clusters.[16] Thus, existing experimental results on the interaction energy are widely scattered from 0.02 (=161 cm^{-1}) to 0.6 eV (=4839 cm^{-1}), suggesting only that Mn_2 is a rather weakly bound molecule.

The *ab initio* calculations performed up-to-date[17–22] have demonstrated that Mn_2 continues to be a challenge to theorists. The first calculation on Mn_2 was carried out by Nesbet[17] at the Hartree–Fock (HF) level using the Heisenberg exchange Hamiltonian [Eq. (2)]. Nesbet found that the ground state is antiferromagnetic with J=−4.1 cm^{-1}, r_e =2.88 Å, and D_e=0.79 eV. The first real post HF calculation appeared 40 years later,[19] indicative of methodological difficulties and lack of appropriate basis sets. Similarly to the case of the Cr_2 dimer[23] a reliable potential curve for Mn_2 cannot be obtained by single reference methods, be it configuration interaction (CI), coupled cluster, or Møller–Plesset perturbation theory, with the exception of the state with the maximum total spin S=5. As was first shown by Bauschlicher[18] the complete active space self consistent field (CASSCF) wave function of the $^1\Sigma_g^+$ state features a pronounced multiconfigurational character. Hence, in order for one to obtain sensible results on the Mn_2 molecule a high level multireference approach is, in general, mandatory.

Wang and Chen[19] calculated potential energy curves (PECs) for all states of Mn_2 dissociating to ground state atoms with total spin S=0–5, namely singlets to undecets, at the CASPT2 level employing effective core potentials. A singlet ground state was found with a binding energy D_e =0.12 eV (=968 cm^{-1}) at r_e=3.64 Å. The minimum of the PECs is shifted to larger internuclear distances and slightly smaller D_e values as we move from singlets (S=0) to undecets (S=5), with the exchange interaction energies $E(S)$ deviating significantly from the Landé rule [Eq. (3)]. It should be noted, however, that the PECs calculated in Ref. 19 are not complete and their spatial symmetries have not been assigned.

The next multireference calculation on Mn_2 was published by Yamamoto *et al.*[20] These authors employed the second order multiconfiguration quasidegenerate perturbation theory developed by Nakano.[24] They consider only states with minimum and maximum total spin, one singlet $^1\Sigma_g^+$ (S=0) and two undecets $^{11}\Sigma_u^+$ and $^{11}\Pi_u$ (S=5). The ground state was found to be of $^1\Sigma_g^+$ symmetry with r_e =3.29 Å and D_e=0.14 eV (=1129 cm^{-1}). Note the large Δr_e=0.35 Å difference in bond length for the $^1\Sigma_g^+$ state in Refs. 19 and 20.

Recently, Negodaev *et al.*[21] performed CASPT2/[6*s*5*p*4*d*3*f*2*g*1*h*] calculations on the six Σ lowest states of Mn_2 correlating to $Mn(^6S)+Mn(^6S)$, singlet to undecet. It was found that from $^1\Sigma_g^+$ to $^{11}\Sigma_u^+$ state D_e values decrease monotonically from 0.28 to 0.24 eV, respectively. By applying the basis set superposition error (BSSE) correction these values reduce to 0.14 and 0.12 eV at r_e(BSSE)=3.40 and 3.55 Å, respectively. It is clear that the results of Ref. 21 cannot be considered as reliable; for one thing the BSSE corrections reduce by half the BSSE free D_e values, which could not be in the case of a relatively large basis set; hence, the results of Ref. 21 are not to be trusted.

Finally, Buchachenko[22] performed restricted coupled-cluster (RCCSD(T)) calculations on the undecet $^{11}\Sigma_u^+$ state in the basis set saturation limit. For the $^{11}\Sigma_u^+$ state he obtained $r_e \approx 3.69$ Å and $D_e \approx 540$ cm^{-1} (=0.0667 eV). These results are the best so far in the literature (*vide infra*).

A large number of calculations on Mn_2 have been performed by the density functional theory (DFT) method.[25–38] The results obtained by different groups differ significantly among each other depending on the functional used. To give just an example, the three functionals LSDA, BPW91, and B3LYP used in Ref. 28 give r_e=1.62, 2.50, and 3.55 Å and D_e=1.54, 0.91, and 0.06 eV, respectively. Most of DFT calculations predict wrongly a ferromagnetic ground state with S=5, although in several DFT studies an antiferromagnetic singlet ground state is also predicted, whereas a triplet ground state is obtained in Ref. 35. In a recent publication by Jellinek *et al.*[38] employing a special DFT procedure,[39] the antiferromagnetic and ferromagnetic states were found competitive with the former winning by 0.002 eV/atom.

The discussion above shows clearly that DFT results on Mn_2 are quite conflicting. One of the reasons of the DFT failure is that all methods used in Refs. 25–38 are of single reference type. Our preliminary calculations showed that in single-reference approaches, even at the RCCSD(T) level, convergence at all internuclear distances and a smooth potential energy curve can be achieved, as expected, only for the $^{11}\Sigma_u^+$ state. On the other hand, unrestricted UCCSD(T) and UMP4(SDTQ) calculations for the same state produce PECs with two minima at r_e=2.58 and 3.40 Å and very unphysical interaction energies at large distances.[40] For the singlet $^1\Sigma_g^+$ state the potential curve obtained at the ROMP2 level has two minima at r_e=1.70 and 2.25 Å and does not converge at small and large distances.[40]

Another reason of the inapplicability of DFT methods to study states with a definite total spin S, stems from the invariance of the Kohn–Sham equations with respect to the total spin S. As was proved in Refs. 41 and 42, the electron density of a N-electron system is invariant with respect to the total spin, therefore the conventional Kohn–Sham equations cannot distinguish states of different spin. The analysis of the existing DFT procedures developed so far for the study of spin-multiplet structures is given in Ref 42. It is shown that all these procedures modify only the expression for the exchange energy and use correlation functionals not corresponding to the total spin of the state. The Mn_2 DFT data[25–38] confirm these theoretical conclusions.[41,42]

In the present work, using multireference variational methods we have constructed two manifolds of PECs, the "ground state" manifold correlating to ground state Mn atoms, ^6S ($4s^23d^5$) and an "excited" one correlating to $Mn(^6S)+Mn(^6D;\ 4s^13d^6)$, with ^6D being the first excited state of Mn. Specifically, we have calculated all PECs corre-

lating to ground state Mn atoms, singlets ($S=0$) to undecets ($S=5$), and six undecets with end products $Mn(^6S)+Mn(^6D)$. We hereafter report bond lengths (r_e), interaction energies (D_e), harmonic frequencies (ω_e), and energy separations (T_e). In addition, an effort has been made to analyze the nature of interaction between the two Mn atoms.

II. METHODOLOGY

For all Mn_2 $^{2S+1}|\Lambda|$ states presently considered the Balabanov–Peterson[43] augmented correlation consistent basis set of quadruple quality, aug-cc-pVQZ $=(23s19p12d4f3g2h)$ was employed, generally contracted to $[9s8p6d4f3g2h]\equiv$A4Z. When correlating the semicore $3s^23p^6$ electrons the A4Z basis was augmented by a series of weighted core functions, resulting to the aug-cc-pwCVQZ $(25s21p14d5f4g3h)$ basis set similarly contracted to $[11s10p8d5f4g3h]\equiv$CA4Z.[43] For two Mn atoms the CA4Z basis comprises 370 spherical Gaussians. This extended basis was employed exclusively for the $^{11}\Sigma_u^+(1)$ state belonging to the $Mn(^6S)+Mn(^6S)$ manifold.

To study all possible spin states, $S=0$ to $S=5$ and to calculate full PECs, a multireference approach is in general mandatory; currently, we have selected the CASSCF +single+double replacements method, CASSCF+1+2 =MRCI.

Our CASSCF reference wave functions for the bundle of the first six, in essence degenerate states (*vide infra*) correlating to two Mn ^6S atoms, were built by allotting the 10 $3d$ electrons to 10 orbitals under C_{2v} constraints. Dynamical correlation was extracted through the CI (valence) MRCI procedure, but from an enlarged reference space including the $4s$ unoptimized orbitals. This approach was followed because by including the two $4s$ orbitals in the construction of the CASSCF wave functions, we were faced with severe technical problems in the subsequent MRCI calculations. The approximation of the internal contraction (ic) (Ref. 44) was applied to make the MRCI valence calculations feasible; for instance, the $^3\Sigma_g^+$ icMRCI expansion, one of the largest, numbers 40×10^6 configuration functions (CF), as compared to $\sim9.3\times10^9$ CFs of the uncontracted space.

Now, the reference wave functions of the six undecet ($S=5$) states correlating to $Mn(^6S)+Mn(^6D)$ (excited manifold) have been constructed by distributing the 14 valence (active) electrons $(4s^23d^5+4s^13d^6)$ to 12 orbital functions, along with the state averaged (SA) technique.[45] Subsequent icMRCI calculations were performed as previously described.

Restricted coupled-cluster calculations RCCSD(T) (Ref. 46) were also performed, but only for the single reference $^{11}\Sigma_u^+(1)$ state.

Scalar relativistic effects were taken into account by the second order Douglas–Kroll–Hess (DKH2) approximation,[47] employing a modified basis set contraction as suggested by Balabanov and Peterson.[43] DKH2 corrections were taken into account only for the lower manifold $^{11}\Sigma_u^+(1)$ state for reasons that will be clear later.

BSSE effects, which have been estimated as usual by the counterpoise method,[48] are less than 0.03 kcal/mol (=10.5 cm^{-1}) for the lowest manifold of states and ranging from 0.07 (=24.5 cm^{-1}) to 0.14 kcal/mol (=49 cm^{-1}) for the higher one.

Finally, size nonextensivity effects were ameliorated by applying the supermolecule approach in the calculation of the interaction energies, in conjunction with the Davidson correction (+Q) (Ref. 49) and the multireference averaged coupled pair functional (ACPF) (Ref. 50) approach. It should be stressed at this point that size nonextensivity is a serious drawback, and this is the case for the CASSCF+1+2 method notwithstanding its advantages over other techniques. For instance, the calculation of the MRCI interaction energy of Mn_2 ($^{11}\Sigma_u^+(1)$) including the 16 semicore $3s^23p^6$ e^- of Mn atoms fails dismally because it cannot cope with $7\times2+8\times2=30$ electrons (*vide infra*).

All calculations were performed with the MOLPRO package.[51]

III. RESULTS AND DISCUSSION

Two $^6S(3d^54s^2)$ ground state Mn atoms give rise to six molecular states of $\Lambda=0$ spatial angular momentum along the intermolecular axis, with spin multiplicities ranging from 1 to 11, namely, $^1\Sigma_g^+$, $^3\Sigma_u^+$, $^5\Sigma_g^+$, $^7\Sigma_u^+$, $^9\Sigma_g^+$, and $^{11}\Sigma_u^+(1)$. With the exception of the $^{11}\Sigma_u^+(1)$, all lower multiplicity states are of extreme multireference character. For instance, for the $^3\Sigma_u^+$ state $\Sigma_{i=1}^{165}|C_i|^2\approx0.9$, where $\{C_i\}$ are the variational coefficients of the MRCI expansion, with the first 165 C_i's ranging from about 0.084 to 0.070. From the same multireference character also suffer the rest of the states but the $^{11}\Sigma_u^+(1)$. Our findings on the lower manifold are discussed in Sec. III A.

As was already mentioned the first excited state of $Mn(^6D)$ is located 2.145 eV above the ground state;[3] at the MRCI(+Q)/A4Z level the ^6D-^6S energy difference is calculated to be 1.99 (2.23) eV in relatively good agreement with experiment. The $Mn(^6S)+Mn(^6D)$ interaction gives rise to states of Σ, Π, and Δ symmetries, with spin multiplicities ranging as before from singlets to undecets ($S=5$). Specifically, we have examined all undecet states of symmetries $^{11}\Sigma_g^+$, $^{11}\Sigma_u^+(2)$, $^{11}\Pi_g$, $^{11}\Pi_u$, $^{11}\Delta_g$, and $^{11}\Delta_u$; these are discussed in Sec. III B.

A. $^1\Sigma_g^+$, $^3\Sigma_u$, $^5\Sigma_g^+$, $^7\Sigma_u^+$, $^9\Sigma_g^+$, and $^{11}\Sigma_u^+(1)$

All states above correlate to two ground state Mn atoms ^6S $(4s^23d^5)$. The mean radii of $3d$ and $4s$ shells are 1.13 and 3.38 bohr, respectively,[52] or $\langle r_{4s}\rangle/\langle r_{3d}\rangle\approx3$, meaning that the $3d^5$ electrons are shielded by the $4s^2$ electron distribution and their overlap in Mn_2 is very small. Therefore, as two ^6S Mn atoms approach each other from infinity one expects a weak, practically spin independent interaction, be it $S=0$, 1, 2, 3, 4, or 5 and this is exactly what we find. Figure 1 displays MRCI PECs of all six states at the MRCI+Q level, whereas Table I collects all our numerical results.

In what follows we discuss our findings starting from the $^{11}\Sigma_u^+(1)$ state, because its single reference character (see below) allowed us to study it more thoroughly, so it can be

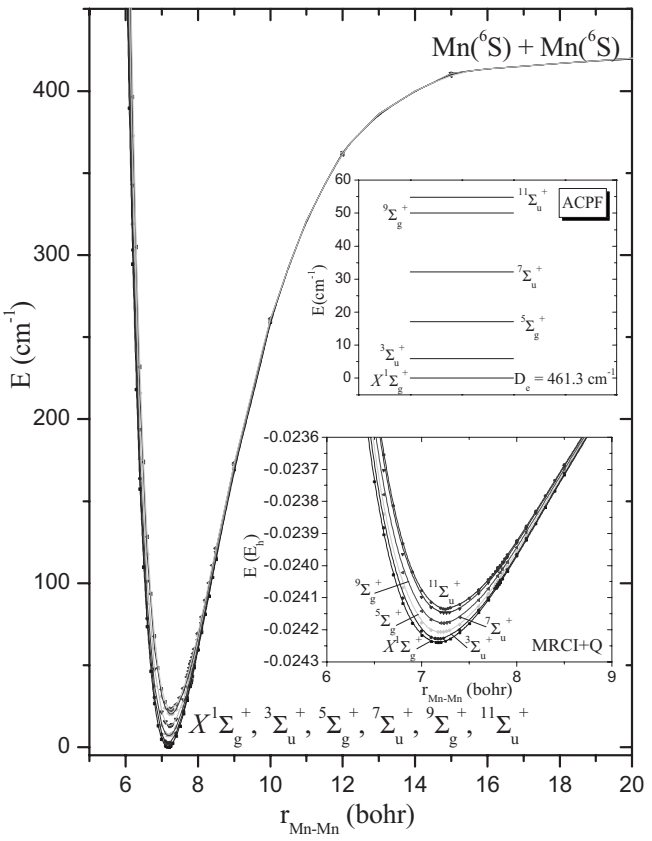

FIG. 1. MRCI+Q/A4Z potential energy curves of the six lowest states of the Mn_2 molecule. Inset 1: MRCI+Q/A4Z potential energy curves around the equilibrium. All energies shifted by $+2300.0E_h$. Inset 2: Corresponding ACPF/A4Z relative energy levels.

used as reference for the lower five states. In addition, we can compare our results with that of Buchachenko[22] who reported high level RCCSD(T) calculations on the $^{11}\Sigma_u^+(1)$ state of Mn_2 using the aug-cc-pVnZ sequence of Balabanov–Peterrson basis sets with $n=3$, 4, and 5, determining D_e at the complete basis set limit, including core correlation and scalar relativistic effects, as well as BSSE corrections.

The leading equilibrium MRCI configuration of the $^{11}\Sigma_u^+(1)$ state is $|^{11}\Sigma_u^+(1)\rangle \approx 0.95|1\sigma_g^2 1\sigma_u^2 2\sigma_g^1 2\sigma_u^1 1\pi_u^2 1\pi_g^2 1\delta_g^2 1\delta_u^2\rangle$ counting only the 14 "valence" electrons of Mn_2.

The best Buchachenko numbers,[22] i.e., RCCSD(T)+core($3s^2 3p^6$) effects+DKH2+CBS, which can be considered as definitive for the $^{11}\Sigma_u^+(1)$ state, are $r_e \approx 3.69$ Å, $D_e(D_0) \approx 540(520)$ cm^{-1}, and $\omega_e \approx 40$ cm^{-1}. These are compared very favorably with our RCCSD(T)/A4Z numbers, i.e., $r_e=3.700$ Å, $D_e(D_0)=529.2(508.3)$cm^{-1}, and $\omega_e=41.8$ cm^{-1} (see Table I). Also, according to Ref. 22, core and relativistic effects combined, reduce the interaction energy by 46.5 (A4Z) or 68.5(A5Z)cm^{-1}, while leaving practically unaltered the bond distance. Therefore, it is clear, that the excellent agreement between our plain RCCSD(T)/A4Z results and that of Ref. 22, is caused by a happy cancellation of correlation and relativistic+core effects.

Continuing our discussion on the $^{11}\Sigma_u^+(1)$ state, Table I shows that the MRCI approach predicts less than half of the D_e and an r_e larger by 0.44 Å, as compared to the RCCSD(T)/A4Z results. The Davidson correction improves the situation, while the multireference ACPF brings the r_e, $D_e(D_0)$, and ω_e in a better agreement with the RCCSD(T) values, i.e., 3.737 Å, 420.4(408.5)cm^{-1}, and 38 cm^{-1}, respectively.

By including the core ($3s^2 3p^6$) electrons ($C-$MRCI/CA4Z), our results diverge further from the RCCSD(T) values, the MRCI method being unable to cope with $(7+8)\times 2=30$ active electrons. Including scalar relativistic effects, D_e diminishes by 3, 12, and 22 cm^{-1} at the C-MRCI+DKH2, C-MRCI+DHK2+Q, and C-ACPF+DKH2 levels, respectively, in analogy with the results of Ref. 22.

The discussion above rationalizes our approach to study all six Mn(^{6}S)+Mn(^{6}S) states at the plain MRCI+Q and ACPF levels, with the latter approach providing semiquantitative results for the $^{11}\Sigma_u^+(1)$ state as compared to RCCSD(T). Hence, scaling uniformly the ACPF interaction energies of the five lower multiplicity states ($2S+1=3-9$) by a factor $s=D_e[\text{RCCSD(T)};{}^{11}\Sigma_u^+(1)]/D_e[\text{ACPF};{}^{11}\Sigma_u^+(1)]=1.26$, and subtracting about 0.04 Å from the bond distances of these states, we strongly believe that our numbers should be close to reality. The scaled results are referred to as s-ACPF in Table I.

The following general conclusions can be drawn from the results presented in Table I. The six Mn(^{6}S)+Mn(^{6}S) states are practically degenerate, densely packed in an energy interval of 0.2 kcal/mol (=70 cm^{-1}). The ground and higher state are of $^1\Sigma_g^+$ and $^{11}\Sigma_u^+$ symmetries with r_e(Å) and D_0(BSSE)(cm^{-1}) values of 3.60 and 554 (s-ACPF) and 3.70 and 494 (RCCSD(T)), respectively. The ordering of states in ascending energy order follows strictly the multiplicity, singlet to undecet, at MRCI+Q, ACPF, and, of course, $s-$ACPF level; even at the plain MRCI level this ordering is discernible.

Another general conclusion is that as we move from the singlet to the undecet state, the Mn–Mn bond length increases monotonically with a total difference range $r_e(^{11}\Sigma_u^+(1))-r_e(X\ ^1\Sigma_g^+)=0.1$ Å at both MRCI+Q and ACPF levels.

In the light of the above, it is rather certain that previous *ab initio* predictions of D_e of the $X\ ^1\Sigma_g^+$ state, namely 968,[19] 1129,[20] and 1129[21] cm^{-1} are about twice as large from the present value, whereas r_e values are underestimated by 0.3 (Ref. 20) and 0.2 Å.[21]

We turn our attention now to the origin of the weak attractive interaction(s) and the role of spin in the Mn(^{6}S)+Mn(^{6}S) manifold of states. The Mn atom having a relatively small nuclear charge ($Z=25$) can be treated nonrelativistically; recall that only in a nonrelativistic approach the total spin S is a good quantum number. In this approximation the total wave function can be written as a linear combination of many-electron spin functions and many-electron coordinate wave functions with permutation symmetry corresponding to the dual Young diagrams.[53] The energy depends on S due to the dependence on S of the coordinate wave function symmetry.[53] As was shown in Ref. 54, it is only the exchange terms that depend on the symmetry of the state, and consequently on the spin, and this dependence is proportional to the orbital overlap integrals. Thus, the smaller the overlap is, the dependence on spin becomes smaller.

TABLE I. Absolute energies E (E_h), bond lengths r_e (Å), binding energies D_e and D_0(BSSE)(cm^{-1}), harmonic frequencies ω_e (cm^{-1}), and energy separations T_e (cm^{-1}) of the low-manifold $Mn(^6S)+Mn(^6S)$ states, singlet ($S=0$) to undecet ($S=5$), at the MRCI, MRCI+Q, and ACPF/AQZ level of theory of the Mn_2 molecule.

State	Method[a]	$-E$	r_e	D_e	D_0(BSSE) [b]	ω_e	T_e
$X\ ^1\Sigma_g^+$	MRCI	2299.995 299	4.128	238.2	218	24.3	0.0
	MRCI+Q	2300.024 239	3.795	426.4	397	36	0.0
	ACPF	2300.028 386	3.644	474.3	440	42	0.0
	s-ACPF[c]		3.60	598	554		0.0
	Expt		3.4[d]	161–4800[e]		68.1,[f] 59[g]	
$^3\Sigma_u^+$	MRCI	2299.995 297	4.130	238.2	218	24.4	0.5
	MRCI+Q	2300.024 228	3.800	424.5	395	36	2.5
	ACPF	2300.028 359	3.652	469.0	436	40	6.0
	s-ACPF[c]		3.61	591	549		7[h]
$^5\Sigma_g^+$	MRCI	2299.995 294	4.132	237.5	217	24.6	1.0
	MRCI+Q	2300.024 207	3.809	419.4	392	34	7.0
	ACPF	2300.028 308	3.669	458.5	425	41	17
	s-ACPF[c]		3.63	578	535		20[h]
$^7\Sigma_u^+$	MRCI	2299.995 290	4.135	236.8	217	24.4	2.6
	MRCI+Q	2300.024 179	3.822	413.4	385	35	13
	ACPF	2300.028 239	3.693	441.2	412	39	32
	s-ACPF[c]		3.65	556	519		42[h]
$^9\Sigma_g^+$	MRCI	2299.995 287	4.138	236.1	216	24.5	2.6
	MRCI+Q	2300.024 147	3.838	406.1	378	35	20
	ACPF	2300.028 158	3.723	426.4	395	38	50
	s-ACPF[c]		3.68	537	498		61[h]
$^{11}\Sigma_u^+(1)$	MRCI	2299.995 291	4.137	237.1	216	24.8	1.8
	MRCI+Q	2300.024 138	3.836	403.6	375	37	22
	ACPF	2300.028 136	3.737	420.4	390	38	55
	s-ACPF[c]		3.70	529	491		69[h]
	RCCSD(T)	2300.034 432	3.700	529.2	494	41.8	
	C-MRCI	2300.736 175	4.692	86.7	73	14	
	C-MRCI+Q	2300.848 915	4.056	274	247	27	
	C-ACPF	2300.876 850	3.809	368	335	35	
	C-MRCI+DKH2	2315.755 479	4.708	83.6	70	14	
	C-MRCI+DKH2+Q	2315.868 962	4.068	262	236	26	
	C-ACPF+DKH2	2315.897 055	3.828	346	314	33	

[a]+Q and DKH2 refer to Davidson correction and to second order Douglas–Kroll–Hess relativistic corrections; C means that semicore correlation effects have been taken into account.
[b]$D_0(\mathrm{BSSE}) \equiv D_e - \omega_e/2 - (\mathrm{BSSE})$.
[c]Scaled ACPF, see text.
[d]References 5 and 6. The experimental r_e ranging from 3.2 (Ref. 6) to 3.8 (Ref. 12).
[e]See text.
[f]Reference 11(a).
[g]Reference 11(b).
[h]Obtained by subtracting s-ACPF D_e values.

As was shown through our numerical results the energy dependence of the $Mn(^6S)+Mn(^6S)$ states on the total spin $S=0-5$ is very small indeed, the reason being that only the $3d$ electrons contribute to the total spin and, as was discussed above, their overlap in Mn_2 is negligible.

According to Eq. (3), the exchange coupling constant J can be obtained from the energy differences between adjacent spin states. In Table II we present the spin energy differences $\Delta_{S,S-1}$ and the corresponding J values calculated at the ACPF level. Although for $S=1-3$ there is no significant variation from the proportionality law, for $S=4$ and especially for $S=5$ the Landé interval rule, Eq. (3), is violated. The average of the exchange coupling constant over all spin states gives $\bar{J}=-4.41\ cm^{-1}$ (after scaling $\overline{J_{sc}}=-5.6\ cm^{-1}$), in close agreement with Nesbet's value $J=-4.13\ cm^{-1}$.[17] In ESR experiments[5] only levels up to $S=3$ were populated. Averaging J over $S=1-3$ states only we get $\bar{J}=-5.53\ cm^{-1}$ ($\overline{J_{sc}}=-6.7\ cm^{-1}$), in fair agreement with the experimental value $J=-9\pm3\ cm^{-1}$.[5]

TABLE II. Energy differences $\Delta_{S,S-1}$ in Mn_2 calculated at the ACPF level.

S (state)	r_e (Å)	$\Delta_{S,S-1}$ (cm^{-1})	$\Delta_{S,\,S-1}/S=-J$
0 ($X\ ^1\Sigma_g^+$)	3.64		
1 ($^3\Sigma_u^+$)	3.65	5.93	5.93
2 ($^5\Sigma_g^+$)	3.67	11.19	5.60
3 ($^7\Sigma_u^+$)	3.69	15.14	5.05
4 ($^9\Sigma_g^+$)	3.72	17.78	4.44
5 ($^{11}\Sigma_u^+(1)$)	3.74	4.83	1.04

TABLE III. Interaction energies at the HF($E_{\text{int}}^{\text{HF}}$) and MRCI($E_{\text{int}}^{\text{MRCI}}$) levels and the correlation energy ($E_{\text{corr}}^{\text{MRCI}}$) of the $^{11}\Sigma_u^+$ state of Mn_2. Bond distances are in a.u. and energies are in kcal/mol.

r	$E_{\text{int}}^{\text{HF}}$	$E_{\text{int}}^{\text{MRCI}}$	$E_{\text{corr}}^{\text{MRCI}}$
15.000	0.000 547	−0.039 016	−0.039 563
12.000	0.019 056	−0.149 200	−0.168 256
10.000	0.145 134	−0.365 680	−0.510 814
9.000	0.375 834	−0.532 569	−0.908 404
8.500	0.599 180	−0.614 795	−1.213 975
8.000	0.955 789	−0.671 087	−1.626 876
7.900	1.050 153	−0.675 702	−1.725 855
7.875	1.075 233	−0.676 354	−1.751 587
7.850	1.100 946	−0.676 781	−1.777 727
7.825	1.127 306	−0.676 975	−1.804 281
7.818	1.134 805	−0.676 986	−1.811 791
7.800	1.154 330	−0.676 925	−1.831 254
7.500	1.538 401	−0.652 484	−2.190 885
7.000	2.525 689	−0.446 657	−2.972 346
6.500	4.275 684	0.213 999	−4.061 686
6.000	7.512 558	1.933 841	−5.578 717
5.500	13.683 676	6.030 803	−7.652 874
5.100	22.571 054	12.797 500	−9.773 554
4.800	33.146 052	21.530 177	−11.615 876
4.600	42.966 281	30.041 853	−12.924 428
4.400	55.825 226	41.583 956	−14.241 270
4.200	72.693 282	57.211 690	−15.481 592
4.000	117.530 770	75.381 114	−42.149 656
3.800	138.801 979	94.056 611	−44.745 368
3.600	168.651 553	120.975 603	−47.675 950

In Table III we present interaction energies of the $^{11}\Sigma_u^+$ Mn_2 state obtained at the HF and MRCI levels along the correlation energy calculated within the spirit of Löwdin's definition[55]

$$E_{\text{corr}}^{\text{MRCI}}(r) = E^{\text{MRCI}}(r) - E^{\text{HF}}(r). \tag{4}$$

It is well known that the physical contributions to the HF energy can be divided into direct electrostatic, exchange, and induction interactions.[56] The ground state Mn atom is of ^6S symmetry; hence, it lacks any electrostatic multipole moments and the electrostatic and induction interactions in Mn_2 have a pure overlap origin from which their short-range character follows. The exchange interaction between the closed inner shells as well the $4s^2$ shell is repulsive, similar to the rare gas dimers. On the other hand as was discussed above, the overlap between the atomic $3d^5$ electrons in Mn_2 is very small, causing in turn a small $3d$-electron exchange interaction, which cannot change the total exchange repulsion.

All these lead to the instability of Mn_2 at the HF approximation. The dimer is stabilized through the attractive electron correlation forces, which at large distances coincide with the dispersion forces; for a numerical proof see Ref. 57. At intermediate distances the dispersion forces cannot be defined without allowing for exchange effects. As follows from Table III, at the equilibrium MRCI distance of the $^{11}\Sigma_u^+$ state r_e=4.137 Å (=7.818α_0), the attractive correlation energy is about 1.6 times larger than the exchange repulsion that provides the stability of Mn_2. The contribution of the electron correlation energy at the ACPF level is even larger. Thus, the only factor of the Mn_2 stability is the electron correlation energy with the dispersion energy being the only attractive factor since the exchange forces are repulsive. Therefore the Mn_2 dimer can be safely attributed to the van der Waals type species.

B. $^{11}\Pi_u$, $^{11}\Sigma_g^+$, $^{11}\Delta_g$, $^{11}\Delta_u$, $^{11}\Sigma_u^+(2)$, and $^{11}\Pi_g$

The interaction of $Mn(^6S_g;\ 4s^23d^5)+Mn(^6D_g;\ 4s^13d^6)$ gives rise to a total of 36 $^{2S+1}|\Lambda|$ molecular states, 18 of *gerade* and 18 of *ungerade* symmetry, singlets to undecets, i.e., $^{1,3,5,7,9,11}(\Sigma_g^+,\ \Pi_g,\ \Delta_g)$ and $^{1,3,5,7,9,11}(\Sigma_u^+,\ \Pi_u,\ \Delta_u)$. Out of these we have studied the six undecets $^{11}\Sigma_{g,u}^+$, $^{11}\Pi_{g,u}$, and $^{11}\Delta_{g,u}$ at the MRCI+Q/A4Z level of theory, not accessible in general through RCCSD(T) or the ACPF approximation. Table IV records all our numerical findings and Fig. 2 displays complete PECs of all six states at the MRCI+Q level, along with the bundle of the lower manifold states previously discussed for comparison.

From the results shown in Table IV it is clear that the interaction between $Mn(^6S)+Mn(^6D)$ atoms is quite differ-

TABLE IV. Absolute energies E (E_h), bond lengths r_e (Å), binding energies D_e and D_0(BSSE) (kcal/mol), harmonic frequencies ω_e (cm^{-1}) and separation energies T_e (kcal/mol) of the higher-manifold of $Mn(^6S)+Mn(^6D)$ undecet states at the MRCI($+Q$)/A4Z level of theory.

State	Method[a]	$-E$	r_e	D_e	D_0(BSSE) [b]	ω_e	T_e
$^{11}\Pi_u$	MRCI	2299.918 010	2.603	15.48	15.1	191.3	48.5
	MRCI+Q	2299.976 604	2.578	25.43	25.0	226	29.9
$^{11}\Sigma_g^+$	MRCI	2299.918 466	2.636	16.17	15.8	189.2	48.2
	MRCI+Q	2299.974 469	2.653	22.99	22.6	203	31.2
$^{11}\Delta_g$	MRCI	2299.898 712	3.101	3.58	3.40	85.2	60.6
	MRCI+Q	2299.951 700	2.891	8.79	8.53	132	45.5
$^{11}\Delta_u$	MRCI	2299.895 975	3.416	1.86	1.74	57.2	62.3
	MRCI+Q	2299.944 794	3.173	4.46	4.3	90	49.9
$^{11}\Sigma_u^+(2)$	MRCI	2299.893 722	3.772	0.64	0.56	29.4	63.7
	MRCI+Q	2299.943 041	3.229	3.27	3.1	85	51.0
$^{11}\Pi_g$	MRCI	2299.894 844	3.703	0.95	0.86	37.4	63.0
	MRCI+Q	22 99.940 557	3.303	2.82	2.65	69	52.5

[a]+Q refers to the Davidson correction.
[b]$D_0(\text{BSSE}) \equiv D_e - \omega_e/2 - (\text{BSSE})$.

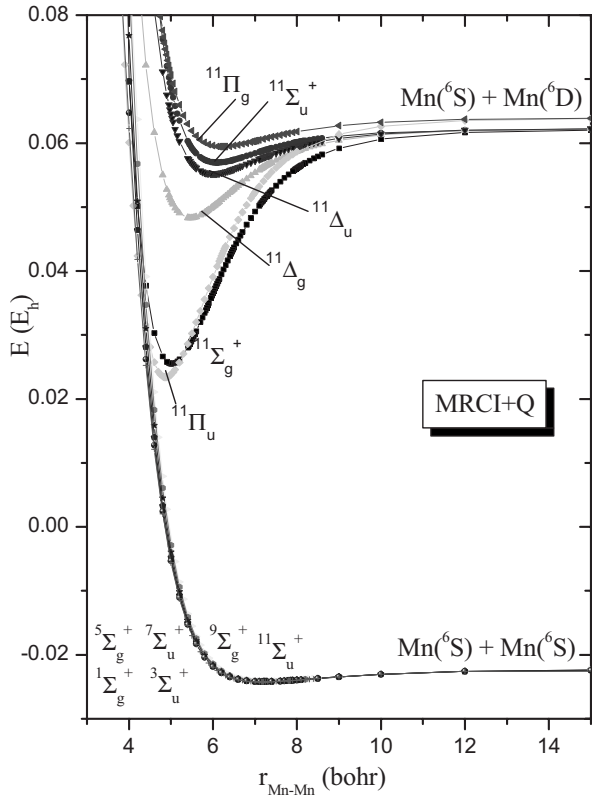

FIG. 2. MRCI+Q/A4Z potential energy curves of 12 states of the Mn_2 molecule. All energies shifted by +2300.0E_h.

ent from the weak van der Waals interaction between two ground state Mn atoms. The Mn(^{6}S)+Mn(^{6}D) interaction leads to chemically bound undecets with binding energies ranging from 25 ($^{11}\Pi_u$) to 2.7 ($^{11}\Pi_g$) kcal/mol, and with a concomitant and monotonic increase and decrease in r_e and ω_e values, respectively as we move from the $^{11}\Pi_u$ to the $^{11}\Pi_g$ state. Note that the $^{11}\Pi_u$ is the ground state of the undecet Mn(^{6}S)+Mn(^{6}D) manifold, located about 30 kcal/mol above the van der Waals states, whereas its companion $^{11}\Pi_g$ is the highest one with $T_e \approx 53$ kcal/mol. To understand better the nature of these states we give their leading equilibrium MRCI CFs along with corresponding Mulliken atomic populations (only valence electrons are counted).

$$|^{11}\Pi_u\rangle \approx 0.89|1\sigma_g^2 1\sigma_u^1 2\sigma_g^1 2\sigma_u^1 1\pi_u^3 1\pi_g^2 1\delta_g^2 1\delta_u^2\rangle 4s^{1.24}4p_z^{0.23} \times 3d_{z^2}^{1.00}3d_{xz}^{1.47}4p_x^{0.03}3d_{yz}^{1.47}4p_y^{0.03}3d_{x^2-y^2}^{1.00}3d_{xy}^{1.00}.$$

$$|^{11}\Pi_g\rangle \approx 0.77|1\sigma_g^2 1\sigma_u^1 2\sigma_g^1 2\sigma_u^1 1\pi_u^2 1\pi_u^3 1\pi_g^2 1\delta_g^2 1\delta_u^2\rangle 4s^{1.42}4p_z^{0.06} \times 3d_{z^2}^{1.00}3d_{xz}^{1.49}4p_x^{0.01}3d_{yz}^{1.49}4p_y^{0.01}3d_{x^2-y^2}^{1.00}3d_{xy}^{1.00}.$$

$$|^{11}\Sigma_g^+\rangle \approx 0.89|1\sigma_g^2 1\sigma_u^1 2\sigma_g^2 2\sigma_u^1 1\pi_u^2 1\pi_u^2 1\pi_g^2 1\delta_g^2 1\delta_u^2\rangle 4s^{1.27}4p_z^{0.22} \times 3d_{z^2}^{1.48}3d_{xz}^{1.00}4p_x^{0.01}3d_{yz}^{1.00}4p_y^{0.01}3d_{x^2-y^2}^{1.00}3d_{xy}^{1.00}.$$

$$|^{11}\Sigma_u^+(2)\rangle \approx 0.74|1\sigma_g^2 1\sigma_u^1 2\sigma_g^1 2\sigma_u^2 1\pi_u^2 1\pi_g^2 1\delta_g^2 1\delta_u^2\rangle 4s^{1.41} \times 4p_z^{0.08}3d_{z^2}^{1.49}3d_{xz}^{1.00}4p_x^{0.01}3d_{yz}^{1.00}4p_y^{0.01} \times 3d_{x^2-y^2}^{1.00}3d_{xy}^{1.00}.$$

$$|^{11}\Delta_g\rangle \approx 0.82|1\sigma_g^2 1\sigma_u^1 2\sigma_g^1 2\sigma_u^1 1\pi_u^2 1\pi_g^2 1\delta_g^3 1\delta_u^2\rangle 4s^{1.33}4p_z^{0.14} \times 3d_{z^2}^{1.00}3d_{xz}^{1.00}4p_x^{0.01}3d_{yz}^{1.00}4p_y^{0.01}3d_{x^2-y^2}^{1.49}3d_{xy}^{1.00}.$$

$$|^{11}\Delta_u\rangle \approx 0.80|1\sigma_g^2 1\sigma_u^1 2\sigma_g^1 2\sigma_u^1 1\pi_u^2 1\pi_g^2 1\delta_g^2 1\delta_u^3\rangle 4s^{1.39}4p_z^{0.08} \times 3d_{z^2}^{1.49}3d_{xz}^{1.00}4p_x^{0.01}3d_{yz}^{1.00}4p_y^{0.01}3d_{x^2-y^2}^{1.00}3d_{xy}^{1.00}.$$

A valence-bond–Lewis diagram of the $^{11}\Pi_u$ (or $^{11}\Pi_g$) state is shown below.

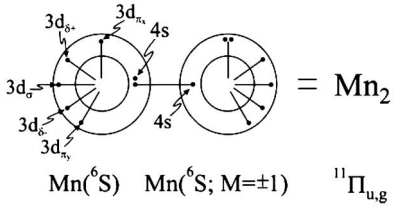

The $^{11}\Pi_u$ leading configuration shows that the bonding is caused through the $4s^2$-$4s^1$ distributions as shown schematically above, with one of the three $4s$-$4s$ electrons promoted to a higher orbital due to the Pauli principle. Moving the $3d_{\pi x}$ ($=3d_{xz}$) electron pair to a $3d_{\delta+}$ ($=3d_{x^2-y^2}$) or $3d_\sigma$ ($=3d_{z^2}$) orbital, the states $^{11}\Delta_{g,u}$ or $^{11}\Sigma^+_{g,u}$ are obtained, respectively.

As seen from Table IV and Fig. 2 the ordering of the states is $^{11}\Pi_u$, $^{11}\Sigma^+_g$, $^{11}\Delta_g$, $^{11}\Delta_u$, $^{11}\Sigma^+_u(2)$, and $^{11}\Pi_g$ with $D_0(\mathrm{BSSE}) \equiv D_e - \omega_e/2 - (\mathrm{BSSE})$ values 25.0, 22.6, 8.5, 4.3, 3.1, and 2.65 kcal/mol, respectively at the MRCI+Q level of theory. According to the atomic Mulliken population analysis the binding energy is proportional to the degree of $4s^p 4p_z^q$, $p+q=1.5$, "hybridization." In ascending energy order from $^{11}\Pi_u$ to $^{11}\Pi_g$ state the (p, q) populations are (1.24, 0.23), (1.27, 0.22), (1.33, 0.14), (1.39, 0.08), (1.41, 0.08), and (1.42, 0.06). Clearly, the smaller the $4s4p_z$ hybridization the smaller the $4s^2$-$4p^1$ overlap, followed by dramatic decrease in the binding energy from 25 ($^{11}\Pi_u$) to less than 3 kcal/mol ($^{11}\Pi_g$) (see Table IV).

Finally, as expected, the bond length r_e increases and the harmonic frequency ω_e decreases regularly from the $^{11}\Pi_u$ to the $^{11}\Pi_g$ state, the differential ranges being $\Delta r_e = 0.73$ Å and $\Delta\omega_e = 157$ cm^{-1}.

It is our hope that the present work will be proved helpful to both experimentalists and theoreticians in the understanding of the electronic structure and bonding of the Mn_2 molecule.

Note added in proof: Since our paper was submitted four new papers on Mn_2 have come to our attention by Camacho *et al.*,[58] Angeli *et al.*,[59] San Mon *et al.*,[60] and Camacho *et al.*[61]

ACKNOWLEDGMENTS

The authors acknowledge Alexei Buchachenko for making available his work (Ref. 22) before publication. The present study was partly supported by the DGSCA Supercomputer Center of UNAM, with grants from CONACyT (Mexico) Grant No. 46770, UNAM Grant No. IN107305, and a special grant from the University of Athens.

[1] C. Demangeat and J. C. Parbelas, Rep. Prog. Phys. **65**, 1679 (2002).
[2] E. Dagotto, in *The Physics of Manganites and Related Compounds*, Springer Series in Solid-State Science, Vol. 136 (Springer, Berlin, 2003).
[3] C. E. Moore, *Atomic Energy Levels*, NSRDS–NBS Circ. No. 35 (U.S. GPO, Washington, D.C., 1971).
[4] D. Chu, C. G. Kenning, and R. Orbach, Phys. Rev. Lett. **72**, 3270 (1994).
[5] C. A. Baumann, R. J. Van Zee, S. V. Bhat, and W. Weltner, Jr., J. Chem. Phys. **78**, 190 (1983).
[6] M. Cheeseman, R. J. Van Zee, H. L. Flanagan, and W. Weltner, Jr., J. Chem. Phys. **92**, 1553 (1990).
[7] M. B. Knickelbein, Phys. Rev. B **70**, 014424 (2004).
[8] J. R. Lombardi and B. Davids, Chem. Rev. (Washington, D.C.) **102**, 2431 (2002).
[9] J. Furthmiller, M. Fähnle, and G. Herzer, J. Magn. Magn. Mater. **69**, 79 (1987).
[10] J. Owen and E. A. Harris, in *Electron Paramagnetic Resonance*, edited by B. Geschwind (Plenum, New York, 1972), Chap. 6.
[11] A. K. Kirkwood, K. D. Bier, J. K. Tompson, T. L. Haslett, A. S. Huber, and M. Moskovits, J. Phys. Chem. **95**, 2644 (1991); K. D. Bier, T. L. Haslett, A. K. Kirkwood, and M. Moskovits, J. Chem. Phys. **89**, 6 (1988).
[12] A. Kant, S. S. Lin, and B. J. Strauss, Chem. Phys. **49**, 1983 (1968).
[13] T. L. Haslett, M. Moscowitz, and A. L. Weitzman, J. Mol. Spectrosc. **135**, 259 (1989).
[14] L. J. LeRoy and R. B. Bernstein, J. Chem. Phys. **52**, 3869 (1970).
[15] K. A. Gingerich, Faraday Symp. Chem. Soc. **14**, 109 (1980).
[16] A. Terasaki, S. Minemoto, and T. Kondow, J. Chem. Phys. **117**, 7520 (2002).
[17] R. K. Nesbet, Phys. Rev. **135**, A460 (1964).
[18] C. W. Bauschlicher, Jr., Chem. Phys. Lett. **156**, 95 (1989).
[19] B. Wang and Z. Chen, Chem. Phys. Lett. **387**, 395 (2004).
[20] S. Yamamoto, H. Tatewaki, H. Moriyama, and H. Nakano, J. Chem. Phys. **124**, 124302 (2006).
[21] I. Negodaev, C. de Graaf, and R. Caballol, Chem. Phys. Lett. **458**, 290 (2008).
[22] A. A. Buchachenko, Chem. Phys. Lett. **459**, 73 (2008).
[23] B. O. Roos, P. R. Taylor, and P. E. M. Siegbahn, Chem. Phys. **48**, 157 (1980).
[24] H. Nakano, J. Chem. Phys. **99**, 7983 (1993).
[25] J. Harris and R. O. Jones, J. Chem. Phys. **70**, 830 (1979).
[26] D. R. Salahub and N. A. Baykara, Surf. Sci. **156**, 605 (1985).
[27] N. Fujima and T. Yamaguchi, J. Phys. Soc. Jpn. **64**, 1251 (1995).
[28] S. K. Nayak and P. Jena, Chem. Phys. Lett. **289**, 473 (1998).
[29] S. K. Nayak, B. K. Rao, and P. Jena, J. Phys. C **10**, 10863 (1998).
[30] M. K. Pederson, F. A. Reuse, and S. N. Khanna, Phys. Rev. B **58**, 5632 (1998).
[31] N. Desmarais, F. A. Reuse, and S. N. Khanna, J. Chem. Phys. **112**, 5576 (2000).
[32] S. Yanagisawa, T. Tsuneda, and K. Hirao, J. Chem. Phys. **112**, 545 (2000).
[33] C. J. Barden, C. C. Rienstra-Kiracofe, and H. F. Schaefer III, J. Chem. Phys. **113**, 690 (2000).
[34] G. L. Gutsev and C. W. Bauschlicher, Jr., J. Phys. Chem. A **107**, 4755 (2003).
[35] M. Valiev, E. J. Bylaska, and J. H. Weare, J. Chem. Phys. **119**, 5955 (2003).
[36] P. Bobadova-Parvanova, K. A. Jackson, S. Srinivas, and M. Horoi, J. Chem. Phys. **122**, 014310 (2005).
[37] M. Kabir, A. Mookerjee, and D. J. Kanhere, Phys. Rev. B **73**, 224439 (2006).
[38] J. Jellinek, P. H. Acioli, J. García-Rodeja, W. Zheng, O. C. Thomas, and K. H. Bowen, Jr., Phys. Rev. B **74**, 153401 (2006).
[39] J. Jellinek and P. H. Acioli, J. Chem. Phys. **118**, 7783 (2003).
[40] U. Miranda and I. G. Kaplan (unpublished results).
[41] I. G. Kaplan, J. Mol. Struct. **838**, 39 (2007).
[42] I. G. Kaplan, Int. J. Quantum Chem. **107**, 2595 (2007).
[43] N. B. Balabanov and K. A. Peterson, J. Chem. Phys. **123**, 064107 (2005).
[44] H.-J. Werner and P. J. Knowles, J. Chem. Phys. **89**, 5803 (1988); P. J. Knowles and H.-J. Werner, Chem. Phys. Lett. **145**, 514 (1988); H.-J. Werner and E. A. Reinsch, J. Chem. Phys. **76**, 3144 (1982); H.-J. Werner, Adv. Chem. Phys. **69**, 1 (1987).
[45] K. Docken and J. Hinze, J. Chem. Phys. **57**, 4928 (1972); H.-J. Werner and W. Meyer, *ibid.* **74**, 5794 (1981).
[46] K. Raghavachari, G. W. Trucks, J. A. Pople, and M. Head-Gordon, Chem. Phys. Lett. **157**, 479 (1989); R. J. Bartlett, J. D. Watts, S. A. Kucharski, and J. Noga, *ibid.* **165**, 513 (1990); **167**, 609E (1990); P. J. Knowles, C. Hampel, and H.-J. Werner, J. Chem. Phys. **99**, 5219 (1993); **112**, 3106E (2000).
[47] M. Douglas and N. M. Kroll, Ann. Phys. (N.Y.) **82**, 89 (1974); B. A. Hess, Phys. Rev. A **32**, 756 (1985); **33**, 3742 (1986); G. Jansen and B. A. Hess, *ibid.* **39**, 6016 (1989).
[48] S. F. Boys and F. Bernardi, Mol. Phys. **19**, 553 (1970); B. Liu and A. D. Mclean, J. Chem. Phys. **59**, 4557 (1973); H. B. Jansen and P. Ros, Chem. Phys. Lett. **3**, 140 (1969).
[49] S. R. Langhoff and E. R. Davidson, Int. J. Quantum Chem. **8**, 61 (1974); E. R. Davidson and D. W. Silver, Chem. Phys. Lett. **52**, 403 (1977).
[50] R. J. Gdanitz and R. Ahlrichs, Chem. Phys. Lett. **143**, 413 (1988); H.-J. Werner and P. J. Knowles, Theor. Chim. Acta **78**, 175 (1990).
[51] MOLPRO, a package of *ab initio* programs written by H.-J. Werner and P. J. Knowles, version 2006.1, R. Lindh, F. R. Manby, M. Schütz, *et al.*
[52] C. F. Bunge, J. A. Barrientos, and A. Bunge, At. Data Nucl. Data Tables **53**, 113 (1993); see also S. P. Walch and C. W. Bauschlicher, in *Comparison of ab initio Quantum Chemistry with Experiment for Small Molecules*, edited by R. J. Bartlett (Reidel, Dordrecht, 1985).
[53] I. G. Kaplan, *Symmetry of Many-Electron Systems* (Academic, New York, 1975).
[54] I. G. Kaplan and O. B. Rodimova, Int. J. Quantum Chem. **7**, 1203 (1973).
[55] P.-O. Löwdin, Adv. Chem. Phys. **2**, 207 (1959).
[56] I. G. Kaplan, *Intermolecular Interactions: Physical Picture, Computational Methods and Model Potentials* (Wiley, Chichester, 2006).
[57] I. G. Kaplan, S. Roszak, and J. Leszczynski, J. Chem. Phys. **113**, 6245 (2000).
[58] C. Camacho, S. Yamamoto, and H. A. Witek, Phys. Chem. Chem. Phys. **10**, 51280 (2008).
[59] C. Angeli, A. Cavallini, and R. Ciriraglia, J. Chem. Phys. **128**, 244317 (2008).
[60] M. San Mon, H. Mori, and E. Miyoshi, Chem. Phys. Lett. **402**, 23 (2008).
[61] C. Camacho, H. A. Witek, and S. Yamamoto, "Intruder states in multireference perturbation theory: The ground state of manganese dimer," J. Comput. Chem.; see http://dx.doi.org/10.1002/jcc.21074.